

CELLULAR RADIOBIOLOGY  
AS APPLIED TO RADIOTHERAPY WITH PARTICULATE RADIATIONS

Paul Todd  
Department of Biophysics  
The Pennsylvania State University

ABSTRACT

The end-point of interest to the radiotherapist is the reproductive death of the cancer cell. This end-point has been extensively studied in vitro using cultured mammalian cells, and much has been learned about the cell-killing ability of charged particle beams. In particular, it has been concluded that beams of negative pions and high energy ions (nitrogen and neon) offer particular advantages to the radiotherapist: maximum effect at maximum depth, little or no exit dose, decreased cellular recovery at maximum depth, and less dependence of the radiation effect upon oxygen at maximum depth. These advantages have been evaluated quantitatively for cultured mammalian cells, and well-defined zones of highly selective tissue destruction are predicted for these beams. Fast neutron beams offer advantages over conventional radiations for therapy due to their enhanced effectiveness for cell killing and less dependence upon oxygen, despite unfavorable depth-effect distribution. High energy protons do not offer the same advantages as high energy heavy ions such as nitrogen and neon.

### Cellular Radiobiology and Radiotherapy

Much has been said about the relevance of the study of the radiation responses of single mammalian cells to the response of tumor cells in the radiotherapeutic situation. I simply wish to point out that many lines of evidence indicate firmly that dose-effect curves (plots of log surviving fraction against absorbed dose, as in Fig. 1) for the survival of cells in tumors resemble those obtained for mammalian cells in culture, using colony formation as the end-point. This resemblance forms the rationale for using mammalian cells in culture to study safely and inexpensively novel radiotherapeutic techniques, including the use of accelerator-produced beams.

### Radiological Physics of Charged Particle Beams

Fast charged particles lose more energy per unit path length as they slow down. I shall use LET to refer to the rate of energy loss (in  $\text{MeV}\cdot\text{cm}^2/\text{g}$ ). This quantity increases with increasing depth (decreasing velocity) and increasing charge of charged particles, as is described in Fig. 2 for heavy ions accelerated by the Berkeley Hilac (Heavy Ion Linear Accelerator). As radiation dose (in rads) is proportional to LET it is clear that dose increases with depth of penetration in charged particle beams.

Also note that the maximum depth of penetration for accelerated B through Ne ions is less than a millimeter. For tissue penetration in excess of 10 cm, beam energies of more than 250 MeV/nucleon are required.

At such high energies, many fast secondary electrons are produced by heavy ions such as nitrogen and neon, so that some cells may experience exposure to conventional radiation instead of the primary beam particle. Thus experiments are necessary to see if the therapeutic advantages predicted by the data I am about to present really exist with high energy heavy ions. Indeed, it can be seen in Fig. 3 that 3.9 GeV nitrogen ions, recently accelerated at the Princeton Particle Accelerator, have the predicted depth-LET relationship.

Negative pi mesons of 50 to 70 MeV have a similarly advantageous depth-LET profile due to the charged particles released in capture reactions at the ends of the pion tracks --"stars". Aside from nuclear reactions in flight, pions interact with matter like electrons until they stop, whereupon their capture by nuclei releases alpha particles (which we shall learn are very effective biologically), protons, neutrons, and other nuclear fragments. Depth dose profiles that result from pion passage through matter have been worked out by Dr. Raju and his collaborators and are presented in detail in Dr. Raju's paper which follows this one. As with heavy ions, a favorable depth-dose pattern is very evident.

#### Effects of Charged Particles on Mammalian Cells

It was discovered by Barendsen in the Netherlands that natural alpha particles near the ends of their tracks are up to 5 times as effective in killing cultured human cells as x rays. Any conditions (chemicals, dose fractionation, oxygen) that changed the responses

of cells to x rays did not change their responses to stopping alpha particles. These discoveries embody significant implications for the therapist. One stopping alpha particle in the cell nucleus leads to reproductive death.

The same observations hold for high LET heavy ions, as indicated in detail in Fig. 4, which depicts dose-response curves for cultured human kidney cells bombarded with 6.6 MeV/nucleon ions from the Berkeley Hilac in the presence and near absence of oxygen. Three differences between heavy ions and x rays are apparent: less survival per unit dose, less dependence upon oxygen, less curvature at low doses. Indeed, when the LET exceeds about  $2000 \text{ MeV-cm}^2/\text{g}$  there is no curvature of the survival curves and no dependence upon oxygen.

It can be seen in the following paper that Dr. Raju has shown a similar set of differences when the killing of cultured cells by stopping negative pions is compared to that of pions in flight.

Some comment about the reduced curvature of the survival curves at high LET is absolutely essential. Purely exponential survival curves imply "one-hit" kill; survival curves with downward curvature imply that sublethal damage must be accumulated to kill. Sublethal damage may be retained or repaired by the cell. It is repaired. If cells that survive a radiation exposure are exposed to a second dose, after a few hours they survive this second dose just as if they had not been irradiated. Multiple exposures of a population of cells, separated by sufficient time for repair, result in survival curves resembling those predicted for 26 MeV helium ions in Fig. 5. These

curves show the cellular counterpart of the sparing effect of dose-fractionation used in radiotherapy. When cell survival curves are purely exponential, there is no such cellular sparing effect of fractionation.

This property of high LET radiations is very important in any discussion of therapeutic use of beams of particles, because dose fractionation schemes can be developed on the basis of anticipated repair at various locations in the beam.

#### Depth-Damage Profiles in Particle Beams

The radiotherapist is interested in the spacial distribution of biological damage in the patient. This he usually predicts on the basis of a three-dimensional depth-dose profile in the form of an isodose plot; this is possible because the relationship between dose and damage is straight-forward when conventional radiations are used. This is not possible with particulate radiations, except electrons and possibly neutrons. In heavy ion and pion beams, dose, oxygen effect, recovery, and killing efficiency all vary with depth. It becomes clear that such concepts as rem dose, dose-equivalent, RBE, radiation quality, etc. are at the pinnacle of their meaninglessness in the assessment of biological damage as a function of depth in a charged particle beam.

Reproductive survival of cells is one measure of biological damage, and it is the only measure for which we have a complete set of data using high LET radiation. Reproductive survival is the end-point of interest to the radiotherapist. Therefore Fig. 6 describes

an exercise that determines the survival of cultured human kidney cells exposed to 100 rads (surface dose) of 230 MeV/nucleon neon ions. The left panel of the figure shows the relevant physical parameters as a function of depth: dose and LET. These parameters were applied to the experimental cell survival curves of Fig. 4, and survival was read from the curves; it was then plotted on the right panel of Fig. 6 to give cell survival as a function of depth in tissue.

A single 100-rad exposure has no use in radiotherapy. If we re-draw all the survival curves in Fig. 4 to look like those in Fig. 5 -- fractionation curves -- then it is possible to obtain depth-survival profiles for therapeutic treatment regimes involving fractionation with cellular recovery, involving hypoxic cells, and involving any kind of particulate radiation of our choosing. Depth-survival profiles can be obtained in this way for pions, neutrons, and gamma rays as well, as long as the appropriate experimental cell survival curves are used. Such curves are available.

A surface dose of 2,000 rads of gamma rays, delivered in 10 equal fractions bears some similarity to a radiotherapeutic regime. This regime leads to a surviving fraction of about  $10^{-3}$  in human kidney cells in culture. Surface doses of gamma rays, neutrons, negative pions, and neon ions that lead to  $10^{-3}$  cell survival are therefore compared in Fig. 7 with respect to the depth-damage profile they produce in 10 cm of cultured human kidney cells (taken as a model patient-tumor system with the tumor centered at 8.5 cm depth). For equivalent surface damage, pions and neon ions produce devastating overkill where gamma rays and neutrons produce less effect than at

the surface. Multiport exposure is therefore necessary with gamma rays and neutrons. The effect of irradiating three fields with these radiations is shown by the fine lines in Fig. 7.

It is more realistic to compare surface doses required for equal tumor damage, assuming a goal of  $10^{-10}$  surviving fraction of cells in the tumor. In the scheme of Fig. 7, if the tumor lacks oxygen and if the radiation is delivered in 10 fields, the accumulated gamma ray surface dose is about 4,000 rads in 200-rad fractions; the accumulated neutron surface dose is about 1/3 of that; and the accumulated pion or neon-ion surface dose is about 100 rads. It appears that, with sensible fractionation, it is possible to expect surface dose reductions up to a factor of 30 when pions or neon ions are used.

#### Prognosis for Biomedical Use of Heavy Ions

The predictions of the previous section assume that LET is a pertinent variable for predicting biological effect. If this assumption is not even a good approximation, then unexpected biological results might be obtained when high energy heavy ions are used to irradiate mammalian cells in culture. Unusual results are not obtained, and the predicted zone of extensive cell killing occurs in cell cultures irradiated with the 3.9 GeV nitrogen ion beam of the Princeton Particle Accelerator, as shown in Fig. 8.

It appears that, with suitable preparatory study, it will be quite possible to adapt high energy nitrogen and neon ion beams to uses involving localized tissue destruction, including treatment of refractory head and neck tumors that are in close proximity to

radiosensitive structures.

Prognosis for Therapeutic Use of Pions and Protons

The similarity of the pion depth-damage profile to that of heavy ions suggests that conclusions drawn about one might also apply to the other. That an attempt will be made to confirm our predictions about pions in the clinical situation is a near certainty, as Dr. Raju points out in his article, which follows.

I have not presented depth-damage profiles for protons, which are naturally of great interest to this symposium. The depth-damage profile for protons will be influenced by range straggling and therefore dependent upon the particle primary energy. If the primary beam energy is 1 GeV or greater, one might predict a rather flat profile. Protons starting at 200 MeV or less, exhibit increased damage at the ends of their tracks in differentiated tissue. Extensive information is available concerning the application of protons to human treatment, and this is the subject of Mr. Koehler's and Dr. Stenson's articles, which follow.



### References

1. T. T. Puck and P. I. Marcus, J. Exptl. Med. 103, 653 (1956).
2. H. B. Hewitt and C. W. Wilson, Nature 183, 1060 (1959).
3. H. D. Suit, R. J. Shalek, and R. Wette, in Cellular Radiation Biology, p. 526 (Williams and Wilkins, Baltimore, 1965).
4. P. Todd, in Second Symposium on Protection against Radiations in Space, p. 107 (U.S. Government Printing Office, Washington, 1965).
5. W. Schimmerling, K. G. Vosburgh, and P. Todd, Science 174, (1971).
6. P. Todd, Radiation Res. Suppl. 7, 199 (1967).
7. P. Todd, "The Prognostic Value of Cellular Studies in Evaluating New Accelerator Beams for Therapy", Los Alamos Scientific Laboratory Report LA-4653-MS (1971).
8. C. A. Tobias and P. Todd, Natl. Cancer Institute Monograph 24, 1 (1967).
9. P. Todd, Radiation Res. 34, 378 (1968).
10. J. J. Broerse, G. W. Barendsen, and G. R. Van Kersen, Intern. J. Radiation Biol. 6, 565 (1968).
11. P. Todd, C. B. Schroy, K. G. Vosburgh, and W. Schimmerling, Science 174, (1971).

### Figure Captions

Figure 1. A - Survival curve of HeLa cells exposed to x rays. The approximate absorbed dose in rads may be obtained by multiplying the abscissa by 1.3. This was the first published survival curve for mammalian cells in culture - determined by Puck and Marcus.<sup>1</sup> Very similar survival curves for ascites tumor cells in mice were first obtained by Hewitt and Wilson.<sup>2</sup>

B - A plot of Tumor volume (right ordinate) against x-ray dose required for an average cure ( $TCD_{50}$ ). The hatched area corresponds to single-cell survival curves that are equivalent to the tumor-cure curve. Work reported by Dr. H. D. Suit et al. from studies of solid rodent tumors of various types.<sup>3</sup>

Figure 2. Particle tracks and Bragg ionization curves of C, N, O, and Ne ions accelerated in the Berkeley Hilac. Based on original data of Dr. T. Brustad.<sup>4</sup>

Figure 3. Stopping-power (LET or  $dE/dx$ ) curve for 3.9 GeV nitrogen ions in polyethylene. Plotted points were differentiated from range-energy relationship determined by time of flight; the solid line is from stopping-power theory.<sup>5</sup>

Figure 4. Survival curves of human kidney T-1 cells irradiated with 6.6 MeV/nucleon heavy ions (ion charge is indicated on each plot).<sup>6</sup>

Figure 5. An example of the effect of dose fractionation on survival curves, demonstrating how fractionation modifies modifying conditions, in this case hypoxia during 26 MeV helium ion irradiation. All curves of Fig. 4 were analysed in this way to obtain the predicted depth-damage profiles calculated in Fig. 7.

Figure 6. Procedure for calculating depth-survival profile following irradiation of human cells with 100 rads of neon ions having 300 MeV/nucleon initial energy.<sup>8</sup> (a) Attenuation of ions in tissue by nuclear collisions. (b) Estimated average single-particle LET. (c) Average LET corrected for collision losses, multiplying (a) by (b). (d) Approximate depth-dose profile due to 100 rads at the surface. (e) Depth-survival profile based on parts (c) and (d) and the cell survival data of Fig. 4. The dashed curve is calculated for anoxic cells, also using survival data of Fig. 4.

Figure 7. Depth-survival profiles for four radiations, applying a  $10^{-3}$  survival dose at the surface. Upper left, 1.3 MeV x rays; upper right, 15 MeV neutrons; lower left, 6 GeV neon ions; lower right,  $45 \pm 5$  MeV negative pions.<sup>7</sup> It is assumed that the entire irradiated zone consists of human kidney T-1 cells or their survival equivalent and that the "tumor" zone lies in the 7 to 10 cm depth interval. Dashed lines indicate hypoxic cell survival, and thin lines

indicate survival after 30 fractions applied in 3 fields in the cases of x rays and neutrons only. Survival data for x rays and heavy ions came from Fig. 4 and related work<sup>9</sup>. Survival data for neutrons came from the studies of Broerse et al.<sup>10</sup> Pion survival data are found in the following article of this series by Dr. M. R. Raju.

Figure 8. Experimental depth-survival profiles for Chinese hamster M3-1 cells irradiated with 3.9 GeV nitrogen ions.<sup>11</sup> Ion fluences were  $6.9 \times 10^6$  (dots),  $1.2 \times 10^7$  (circles),  $2.4 \times 10^7$  (squares), and  $3.2 \times 10^7$  particles/cm<sup>2</sup> (triangles). The data cover the last 2.6 cm. of the beam path.

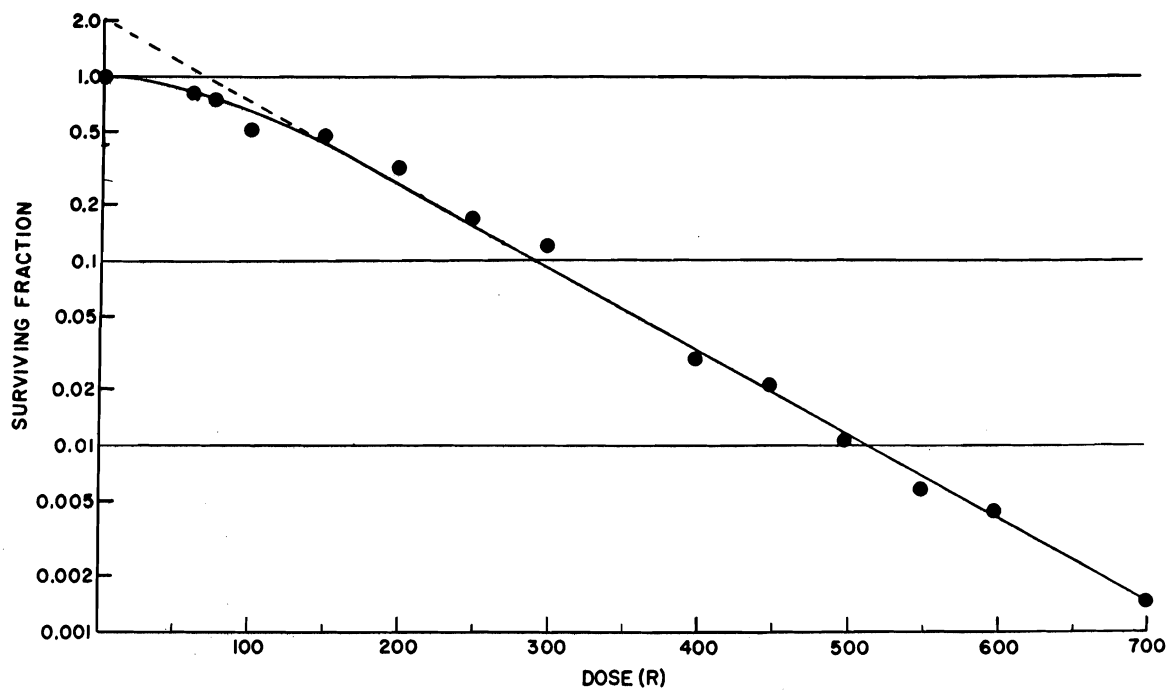


Fig. 1A

LOG<sub>10</sub> CALCULATED SURVIVAL FRACTION VS. TCD<sub>50</sub>

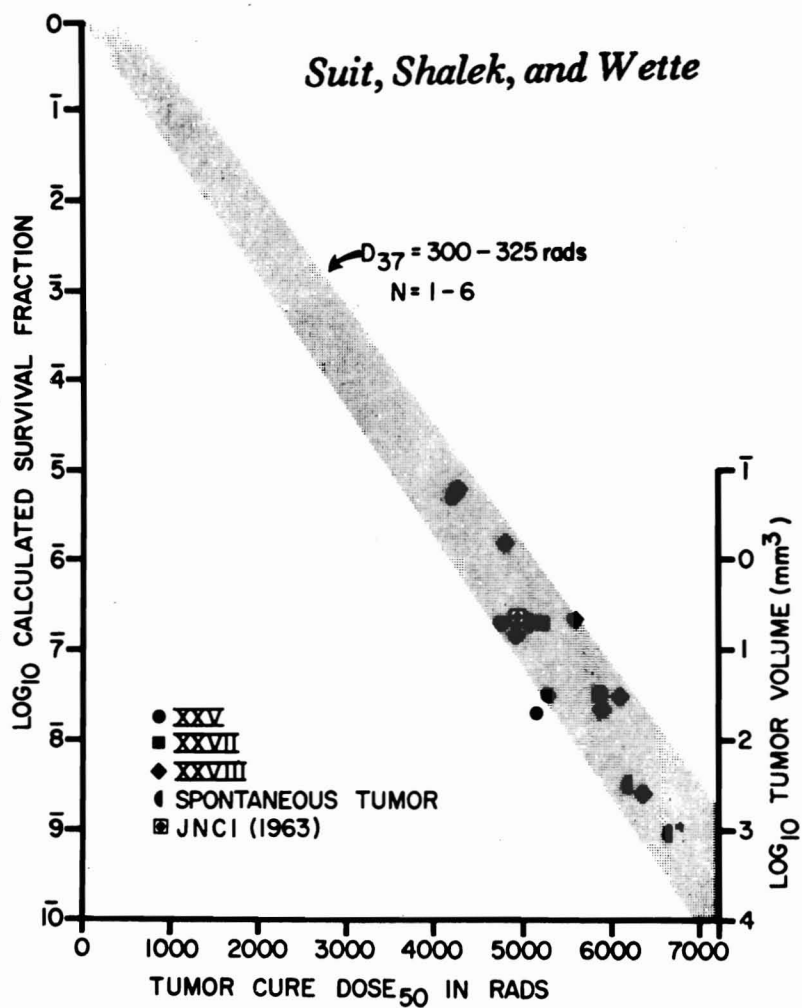


Fig. 1B

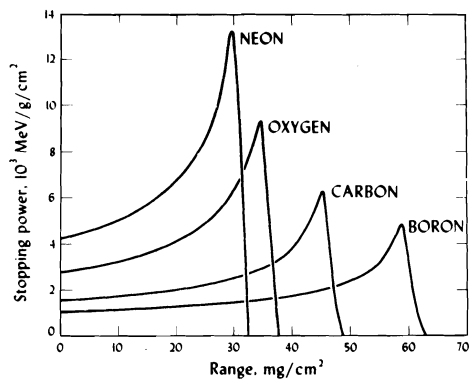
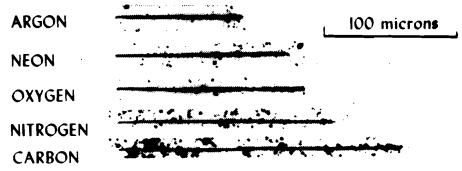


Fig. 2

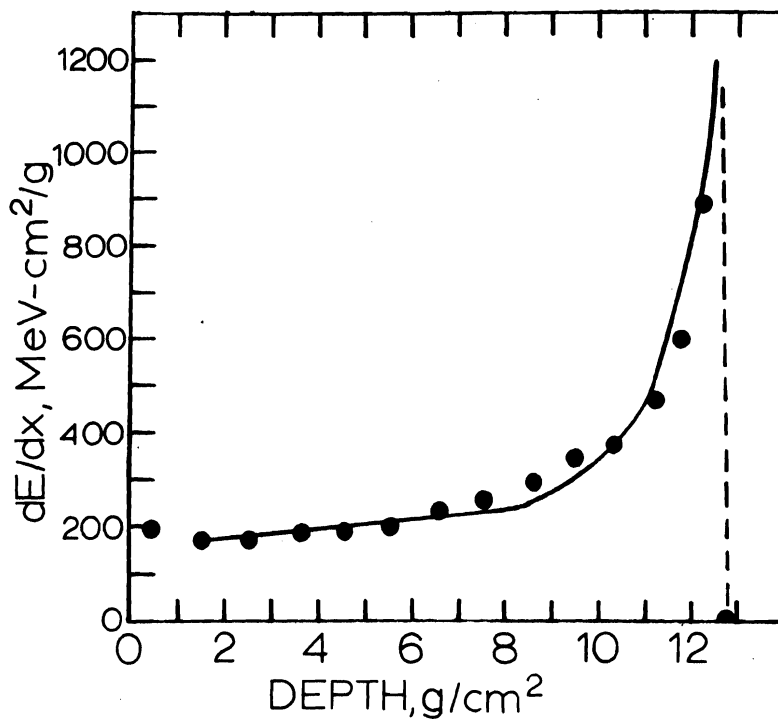


Fig. 3



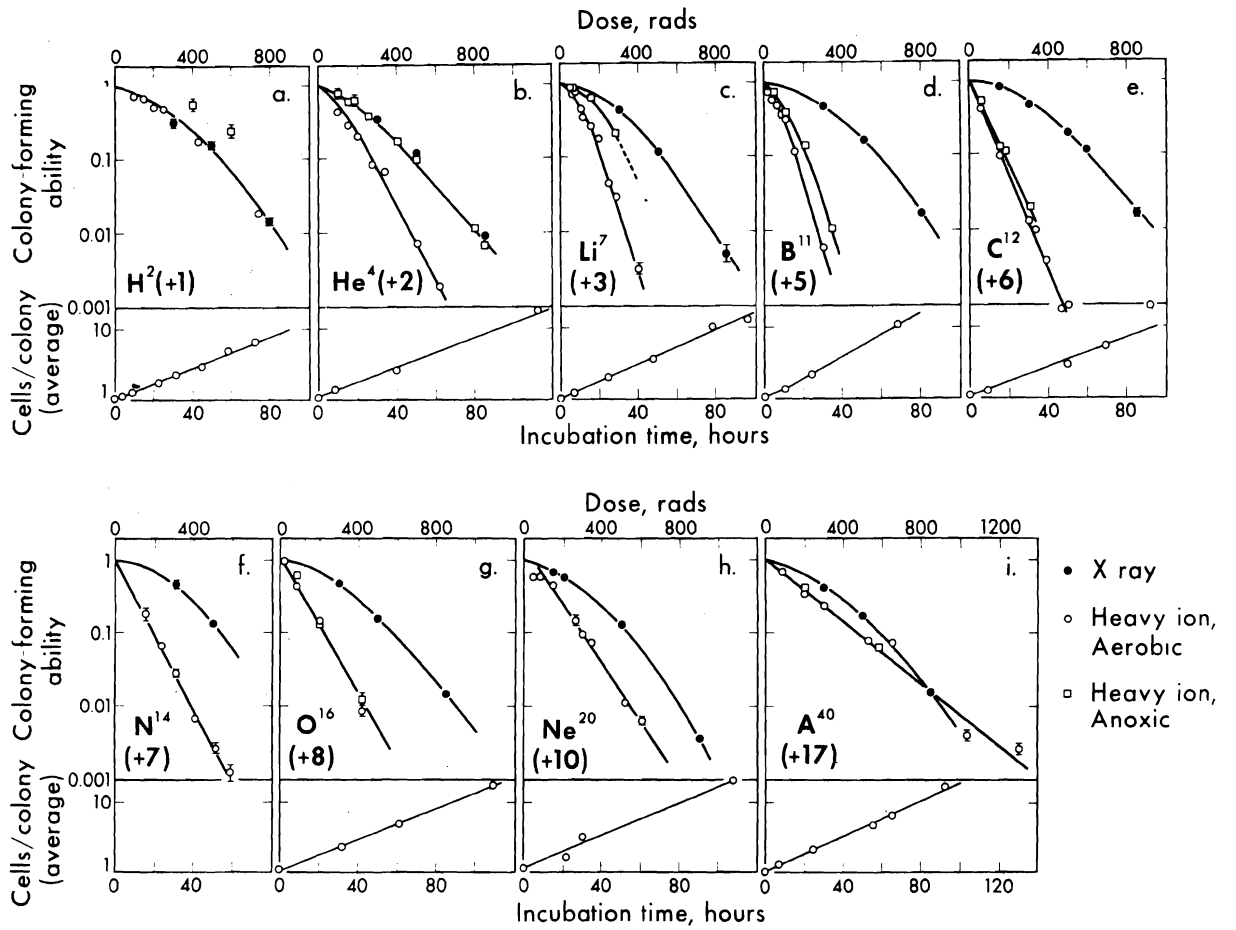


Fig. 4

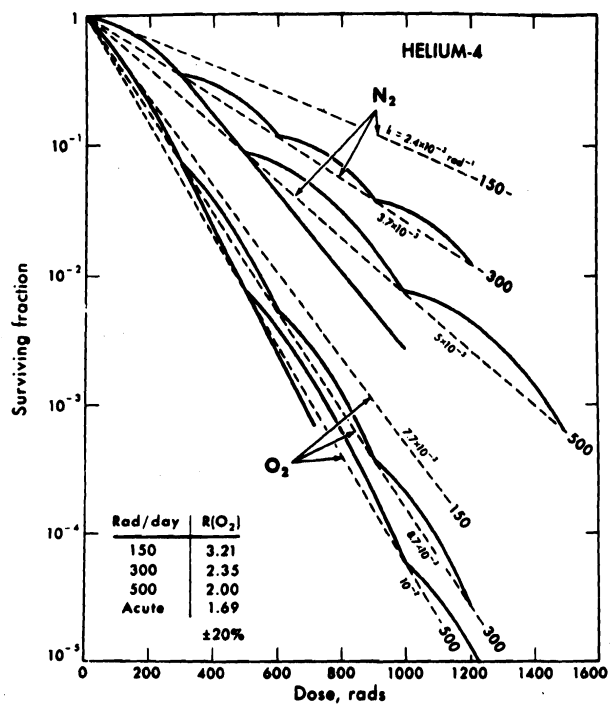


Fig. 5

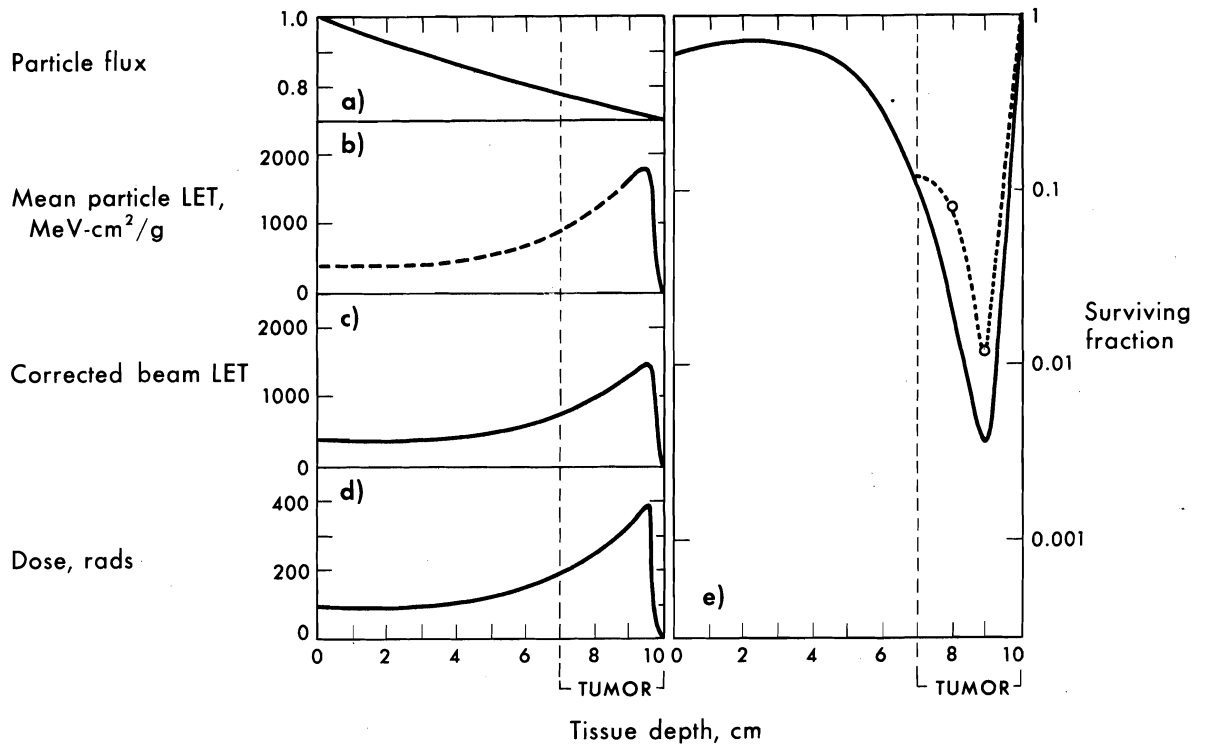


Fig. 6

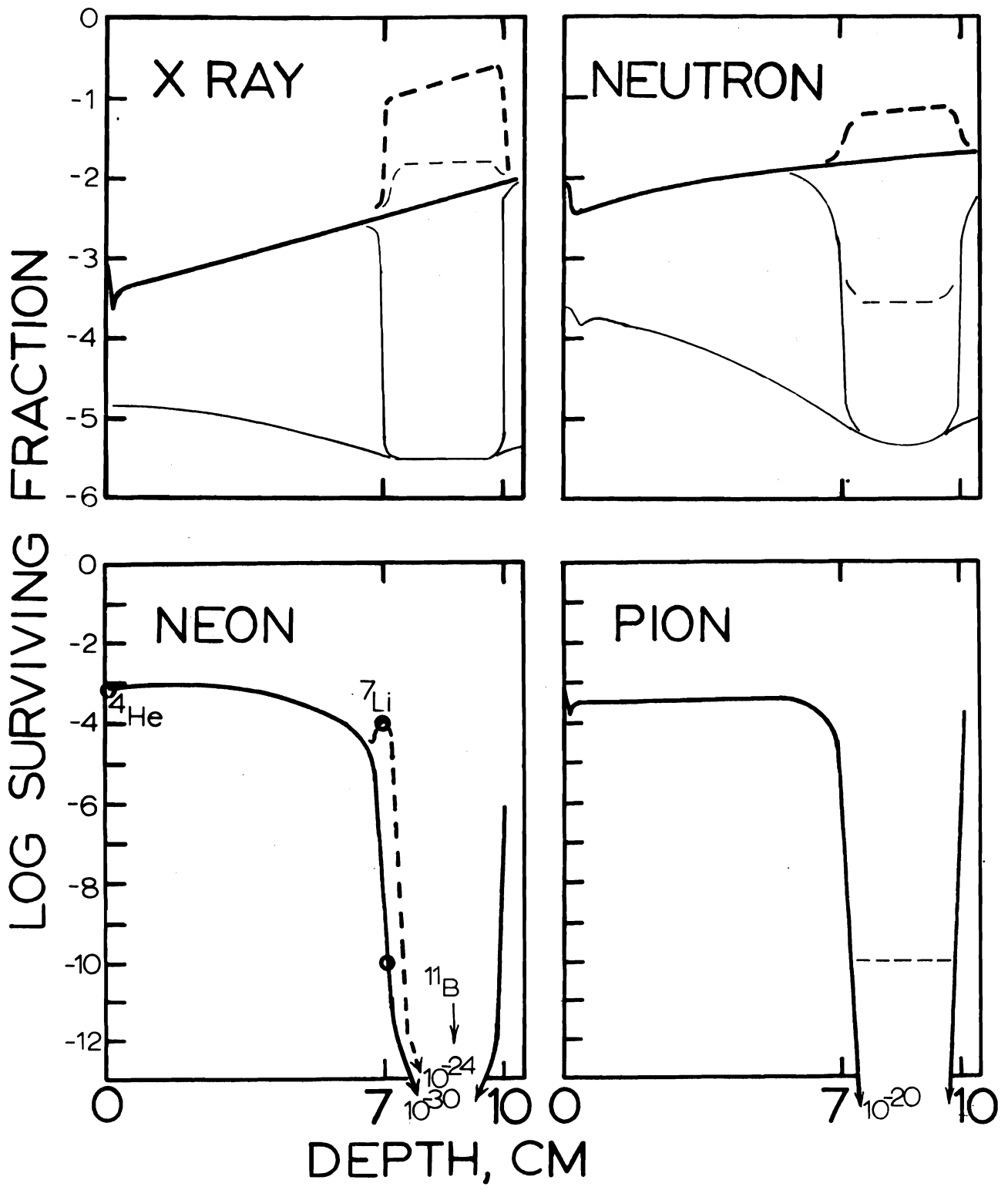


Fig. 7

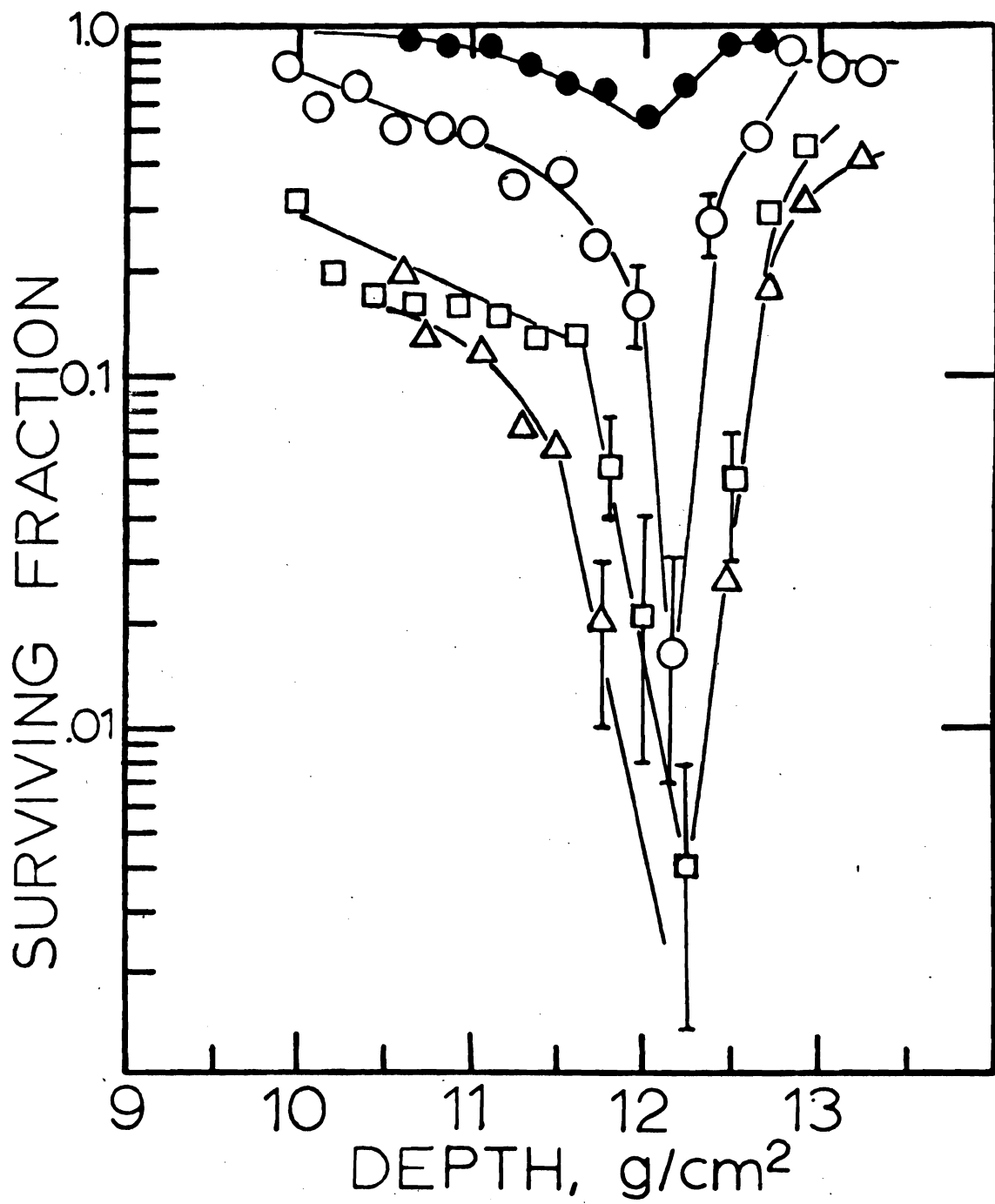


Fig. 8



Vertical text or markings on the right edge, possibly a page number or reference code.



Vertical text or markings on the right edge, possibly a page number or reference code.

